Check for updates

DATA NOTE

ERIES-REVAULTS Pseudo-Dynamic tests on a full-scale masonry cross vault system: dataset

[version 1; peer review: 2 approved with reservations]

Chiara Calderini[1], Sinan Acikgoz[2], Nicoletta Bianchini[3], Chiara Cirabisi[1], Chiara Ferrero[1,4], Paulo B. Lourenço[5], Nuno Mendes[5], Marco Pavesi[6], Giulio Lucio Sergio Sacco[1], Marialuigia Sangirardi[2], Marco Lamperti[7], Marco Peroni[7], Francisco Javier Molina[7], Simone Peloso[7]

[1]University of Genoa, Genoa, Liguria, Italy
[2]University of Oxford, Oxford, England, UK
[3]University of West London, London, England, UK
[4]Delft University of Technology, Delft, South Holland, The Netherlands
[5]University of Minho, Guimaraes, Braga, Portugal
[6]Kerakoll S.p.A., Sassuolo, Emilia-Romagna, Italy
[7]European Commission Joint Research Centre Ispra, Ispra, Lombardy, Italy

v1 **First published:** 08 Sep 2026, **6**:328
https://doi.org/10.12688/openreseurope.23910.1
Latest published: 08 Sep 2026, **6**:328
https://doi.org/10.12688/openreseurope.23910.1

Abstract

This paper presents the dataset generated within the ERIES-REVAULTs experimental campaign, aimed at investigating the in-plane shear behaviour of masonry cross vaults, representative of historic churches. In post-earthquake surveys, the damage associated with this type of mechanism is frequently observed as it is caused by the differential longitudinal displacements of vaults' supports. To investigate this behaviour, a full-scale masonry specimen was constructed at the European Laboratory for Structural Assessment (ELSA), Joint Research Centre (JRC), Ispra, Italy, and tested using Pseudo-Dynamic (PsD) testing technique, to reproduce the seismic action.

The experimental campaign included an initial testing phase on the as-built specimen during which a seismic action was applied. Then, repair, strengthening with a Steel-Reinforced Grout (SRG) system and a second testing phase under the same seismic input conditions followed.

The paper includes information on the specimen's geometry, its construction details, materials, strengthening intervention, test setup, actuators configuration, instrumentation and loading protocols. Most

Open Peer Review

Approval Status ? ?

	1	2
version 1 08 Sep 2026	? view	? view

1. **Maria Cristina Porcu**, University of Cagliari, Cagliari, Italy

2. **Osama Amer**, Institute for Sustainability and Innovation in Structural Engineering (Ringgold ID: 451178), Guimarães, Portugal
Cairo University / Ain Shams University, Cairo, Egypt

Any reports and responses or comments on the article can be found at the end of the article.

of this information is also included in the shared dataset.

Keywords
Historic structures, Brick Masonry Vault, Stone Masonry, Seismic Retrofit, Seismic Behaviour, Pseudo-Dynamic, Hybrid Testing

This article is included in the Joint Research Centre gateway.

This article is included in the Horizon Europe gateway.

Corresponding author: Chiara Cirabisi (CHIARA.CIRABISI@EDU.UNIGE.IT)

Author roles: Calderini C: Conceptualization, Project Administration, Supervision; **Acikgoz S**: Investigation; **Bianchini N**: Conceptualization, Supervision; **Cirabisi C**: Writing – Original Draft Preparation; **Ferrero C**: Conceptualization, Writing – Original Draft Preparation; **Lourenço PB**: Conceptualization, Supervision; **Mendes N**: Conceptualization, Investigation, Supervision; **Pavesi M**: Resources; **Sacco GLS**: Investigation; **Sangirardi M**: Investigation; **Lamperti M**: Data Curation, Investigation; **Peroni M**: Data Curation, Investigation; **Molina FJ**: Data Curation, Investigation; **Peloso S**: Data Curation, Investigation, Writing – Original Draft Preparation

Competing interests: No competing interests were disclosed.

Grant information: This project has received funding from the Horizon Europe Framework Programme under grant agreement No [101058684](Engineering Research Infrastructures for European Synergies [ERIES]).
The funders had no role in study design, data collection and analysis, decision to publish, or preparation of the manuscript.

Copyright: © 2026 Calderini C *et al*. This is an open access article distributed under the terms of the Creative Commons Attribution License, which permits unrestricted use, distribution, and reproduction in any medium, provided the original work is properly cited.

How to cite this article: Calderini C, Acikgoz S, Bianchini N *et al.* **ERIES-REVAULTS Pseudo-Dynamic tests on a full-scale masonry cross vault system: dataset [version 1; peer review: 2 approved with reservations]** Open Research Europe 2026, **6**:328 https://doi.org/10.12688/openreseurope.23910.1

First published: 08 Sep 2026, **6**:328 https://doi.org/10.12688/openreseurope.23910.1

Introduction

The experimental campaign of the ERIES-REVAULTs project was designed to investigate the behaviour of cross vaults subjected to seismic loading. In particular, this study focused on cross vaults located in the lateral naves of three-nave historic churches. These vaults are typically supported on one side by the piers, separating the lateral nave from the central nave, and on the other side by the perimeter wall. The difference in stiffness between these two supports leads to differential longitudinal displacements during earthquakes, causing in-plane shear mechanism on the cross vaults. This type of mechanism was investigated in previous studies by experimentally testing vaulted specimens under static or dynamic actions (e.g.,[1,2,3,4,5]). While these studies provided valuable insights into the in-plane shear response of masonry cross vaults, they primarily focused on the vaults themselves, discarding/neglecting their interaction with the supporting structures.

To address this gap, ERIES-REVAULTs project constructed and tested under seismic actions a full-scale specimen representing an intermediate bay of the lateral nave of a generic three-nave historic masonry church.

The specimen was tested under seismic loading using the Pseudo-Dynamic (PsD) testing technique at the European Laboratory for Structural Assessment (ELSA) at the Joint Research Centre (JRC) in Ispra, Italy. Following the first testing phase, the specimen was strengthened with a Steel-Reinforced Grout (SRG) system applied at the vault and arches extrados and subsequently retested under the same loading conditions to evaluate the effectiveness of the strengthening intervention.

The present paper aims at introducing the relevant information regarding the specimens, measuring equipment, test setup and test procedure of the ERIES-REVAULTs experimental campaign.

Description of the specimens

As-built specimen

The full-scale specimen, illustrated in Figure 1, consists of two stone masonry walls (Wall 1 and Wall 2) supporting a brick masonry cross vault.

The construction phase lasted approximately two months, starting in early June 2025 and concluding in early August 2025. The specimen is built upon a reinforced concrete foundation, with a layer of mortar placed between the foundation

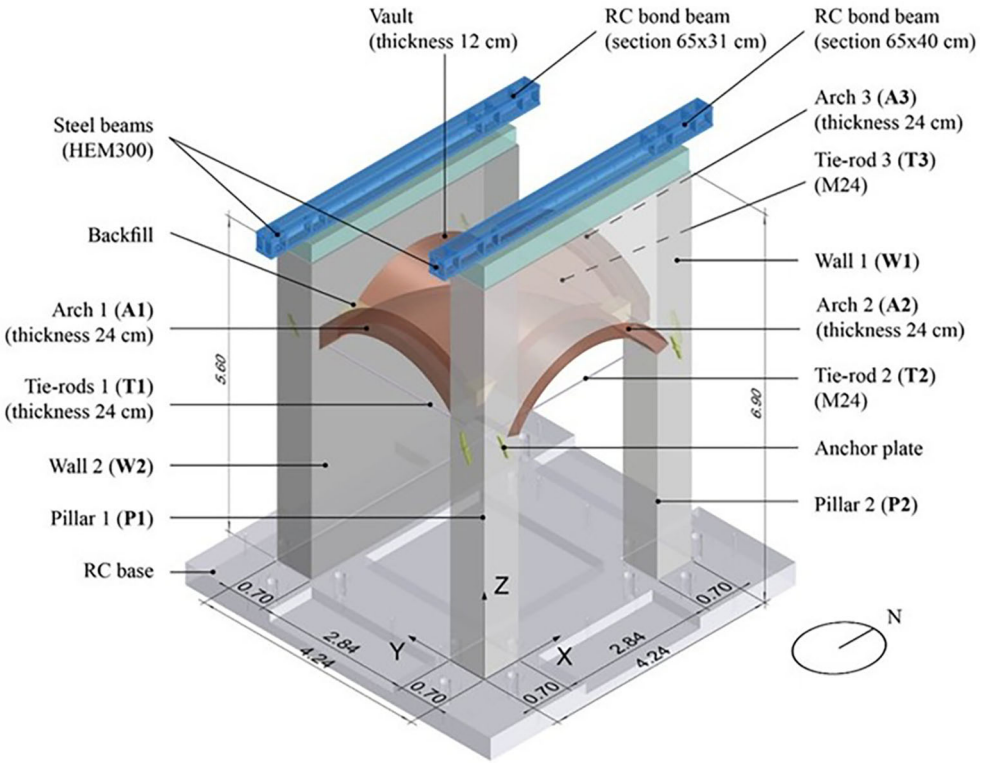


Figure 1. 3D view of the full-scale specimen (dimensions in m).



Figure 2. Brick masonry arrangement: a) extrados view, b) brick arrangement of the transverse arches.

and the base of the pillars (Pillar 1 and Pillar 2) and of the external wall (Wall 2). The brick masonry cross vault, located at a height of approximately 4 m above the foundation, is bounded on three sides by the arches, two transverse (Arch 1 and Arch 3) and one longitudinal (Arch 2), while the fourth side is bounded by the external wall (Wall 2). Structurally, the vault is supported by both the pillars of the internal wall (Wall 1) and the external wall (Wall 2). At its corners, the vault is toothed into these supporting elements, establishing a mechanical interlocking. The connections between the vault and the arches vary along the perimeter of the vault. In fact, a continuous structural connection exists between the vault and the transverse arches (Arch 1 and Arch 3) along their entire length, while the connection between the vault and both the longitudinal arch (Arch 2) and the external wall (Wall 2) is limited near the springing, introducing a structural discontinuity.

Regarding the materials, the vault and arches are constructed using hand-made solid clay bricks with approximate dimensions of 24 × 12 × 6 cm. The bricks are bonded using a pre-mixed natural hydraulic lime mortar of class M5 (BioCalce Pietra, Kerakoll). The vault is built as a single layer of bricks laid on edge and arranged radially (Figure 2a). The arches, on the other hand, have a transverse cross-section characterised by the brick arrangement shown in Figure 2b, in which bricks with their longest side oriented along the radial plane alternate with two superimposed bricks laid on edge.

At the extrados of the vault, four backfills are constructed at the corners. These consist of stacked brick fragments arranged in multiple layers and bonded with the same mortar used in the brick masonry. Notably, these backfills are not structurally connected to the vault or the adjacent walls.

The vertical walls are built using stone masonry composed of limestone extracted from the Saltrio quarry in the Varese province, Italy.[6] The stones are roughly cut, with maximum dimensions ranging from 25–30 cm along the longest side and 15–20 cm along the other sides. They are bonded with the same mortar used for the bricks, enriched with quartz filler,



Figure 3. Stone masonry arrangement: a) transverse face of the pillar, b) transverse face of the wall (Wall 2), c) external face of the wall (Wall 2).

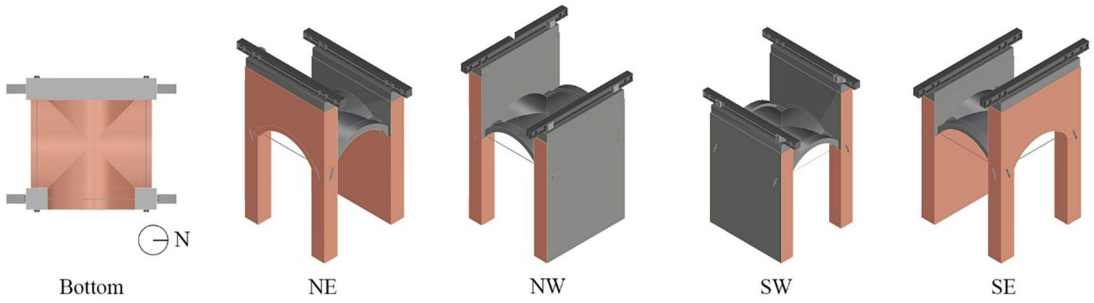


Figure 4. Scheme of the plastered surfaces (in orange).

to reduce its compressive strength, and with gravel (4-6 mm). The wall cross-sections are characterised by larger stones placed on the perimeter and smaller stones filling the inner core. The external arrangement of the stones is illustrated in Figure 3.

Some parts of the specimen, highlighted in orange in Figure 4, are plastered. The intrados of the vault is plastered with a 5 mm thick mineral-based finishing plaster, while the stone masonry surfaces are plastered with an inner layer made of the same pre-mixed natural hydraulic lime used for the mortar, with the addition of gravel, and finished with the mineral-based finishing plaster. The plaster layers for stone masonry are approximately 10–15 mm thick.

A system of steel tie-rods, consisting of M24 threaded rods connected to the stone masonry walls metallic anchor plates, are placed just below the springing level of the arches. All the rods and the anchor plates are made of modern steel.

Finally, at the top of both walls (Wall 1 and Wall 2), a reinforced concrete bond beam made of low-strength concrete is placed, together with a steel beam (HEM300) required to attach the actuators to the specimen. The interface between the masonry and the bond beam is intentionally enhanced by leaving the course of stones partially unfilled with mortar, thereby allowing the concrete to penetrate and create a mechanical interlock. Steel connectors are then used to link the concrete bond beams to the overlying steel beams. Figure 5 shows the specimen after the construction.



Figure 5. Photograph of the specimen after construction: a) south-east view; b) north-west view.

Strengthened specimen

The structural strengthening intervention, carried out after the first set of PsD tests, was carried out in mid-January 2026. The works involved both the intrados and extrados surfaces of the cross vault and consisted of the installation of a Steel-Reinforced Grout (SRG) system, provided by Kerakoll. In particular, the system used is composed of a unidirectional fibre sheet, made of steel micro-cords and fixed to a fibreglass micromesh (Geosteel G600) combined with a M15 geo-mortar (GeoCalce F Antisismico).

The intervention was performed first treating the existing cracks in the cross vault by mechanically opening and subsequently sealing them at the intrados using the geo-mortar. Subsequently, a fluid grout prepared with the same mortar was poured from the extrados to ensure complete filling of the openings and to restore the continuity of the masonry.

After this first phase, the SRG strengthening system was applied to the extrados according to the scheme shown in Figure 6. The system consisted of an initial layer of mortar, with a thickness of approximately 3–5 mm, onto which the fibre sheet reinforcement was placed while the mortar was still fresh. The reinforcement was then covered with a second mortar layer with a thickness of approximately 3–5 mm to protect the fibre sheets.

The fibre sheets applied along the transverse arches were mechanically anchored to the adjacent walls by drilling three holes into the masonry and inserting the cut ends of the sheets into the holes for an anchorage length of approximately 30 cm.

Material properties

To characterise the mechanical properties of the materials employed in the construction of the specimen, both destructive and non-destructive tests were conducted on masonry units as well as on assembled masonry. These properties are essential for the interpretation of the experimental results and for the calibration of the numerical models. In this section, only the main results are briefly reported and they are summarised in Table 1.

The properties of the Saltrio stone are taken from the literature,[6] while brick properties are derived from experimental tests. The results show that Saltrio stone exhibits high stiffness and strength, with both dynamic and static elastic moduli in the range of 60–70 GPa and compressive strength exceeding 100 MPa. The clay bricks show significantly lower strength, with compressive strength around 16 MPa.

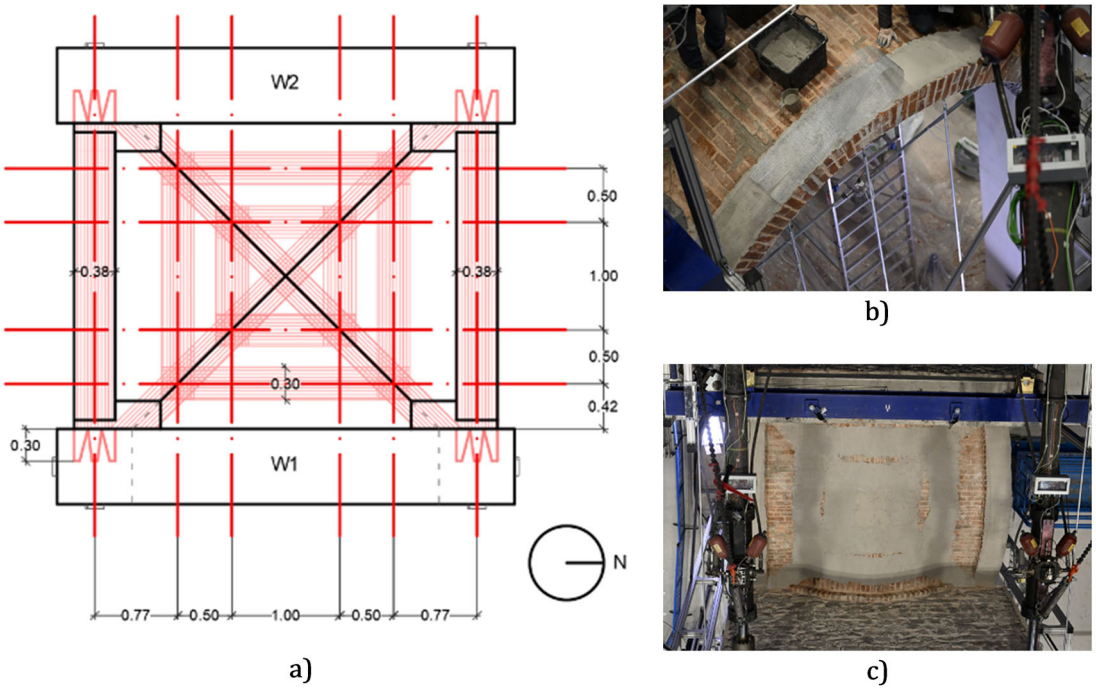


Figure 6. a) Application scheme of the SRG system at the extrados (dimensions in m); b) photograph of the application of the fibre sheet at the extrados of the transverse arch; c) photograph of the completed strengthening intervention.

Sonic tests were conducted at the masonry level, on the external stone wall (Wall 2), on stone pillars (Pillar 1 and Pillar 2) and on the brick vault and arches to derive *in-situ* estimates of the dynamic Young's modulus of masonry.

Both direct and indirect sonic test configurations were adopted, with multiple measurement paths along the height and span of the elements. The measured pulse velocities, combined with assumptions on material density, were used to back-calculate dynamic moduli. The results are summarised in Table 2.

Dynamic identification tests

Dynamic identification tests were performed on the as-built and strengthened configurations through ambient vibration tests under laboratory conditions. It is worth recalling that the previously mentioned reinforced concrete and steel beams were present at the top of the two walls during the dynamic identification tests. The setup included piezoelectric accelerometers (10 V/g sensitivity) and a data acquisition system with a sampling frequency of 200 Hz. During testing, the specimen was simply supported at the base and free at the top. The experimental data were postprocessed using Artemis Modal.

For the as-built configuration, the accelerometer layout is shown in Figure 7, and nine relevant modes were identified in the frequency range between 4.98 Hz and 93.07 Hz (Figure 8).

For the dynamic identification tests performed on the strengthened configuration, the same boundary conditions were maintained (simply supported at the base and free at the top), and ambient vibration tests were carried out under the same laboratory conditions. The accelerometers were positioned in the same locations of the as-built configuration (Figure 7). In this case, eight modes were identified within the frequency range of 4.40–58.69 Hz (Figure 9). Based on the analysis of the mode shapes and the comparison of the MAC values between the as-built and strengthened configurations, the modal sequence remains unchanged, with the exception of modes 5 and 6, which appear inverted in the strengthened configuration. In addition, a general decrease in frequencies is observed, and mode 9 could not be identified in the strengthened configuration. A detailed discussion of the comparison between the as-built and the strengthened configuration is beyond the scope of the present work and is therefore not addressed here.

The experimental campaign

The experimental campaign aimed at evaluating both the response of the as-built structure and the effectiveness of the strengthening intervention based on Steel Reinforced Grout (SRG) technique, by structuring the campaign in two main phases. In the first phase, the specimen was tested in its as-built configuration, while in the second phase, after the application of the SRG strengthening system, the specimen was re-tested under the same loading conditions.

The experimental investigation was conducted under displacement-controlled conditions, with two independent horizontal longitudinal Degrees of Freedom, DoF1 and DoF2, applied at the top of the walls (Figure 10). This configuration

Table 1. Results of destructive and non-destructive tests carried out on stone and brick units.

Material	Test type	No. of specimens	Mean value(s)	Standard(s)
Saltrio stone	Apparent density, open porosity	6	$\rho_\beta \approx 2690$ kg/m^3; $\rho_o \approx 0.4$	EN 1936:2006
	Dynamic modulus (UPV)	19 (⊥ and//)	$E_d \approx$ 63-70 GPa (direction-dependent)	
	Static modulus in compression	19	$E_s \approx$ 62-71 GPa	EN 12390-1, -2
	Compressive strength	19	$f_c \approx$ 114-157 MPa (orientation-dependent)	EN 12390-1, -2
	Flexural tensile strength	–	$f_{tc,f} \approx 18.6$ MPa	EN 12372:2022
	Splitting tensile (Brazilian)	–	$f_{tc,B} \approx 6.46$ MPa	EN 12390-6 (by analogy)
Clay bricks	Flexural tensile strength	11	$f_t \approx 6.18$ MPa	EN 772-1
	Compressive strength	22	$f_c \approx 15.8$ MPa	EN 772-1
	Physical properties	–	$\rho \approx 1620$ kg/m^3; size 6 × 12 × 24 cm	

Table 2. Dynamic Young's modulus of stone and brick masonry derived from sonic test results.

Structural Element	Materials	n (pairs × velocities) *	Test type	Dynamic Young's Modulus [GPa]		
				min-max	AVG	COV
Wall 2	Stone	4 × 20	Direct tests	5.8 – 13.6	9.6	36%
Pillar 1/Pillar 2	Stone	2 × 20	Direct tests	9.0-12.9	9.9	26%
		2 × 20	Indirect tests	10.4-18.7	13.7	34%
Vault and Arch 3	Brick	2 × 20	Direct tests	2.6-4.4	3.5	36%
		2 × 20	Indirect tests	2.6 – 5.1	3.9	44%

*n = number of measurement paths (point pairs) × number of repeated pulse velocity measurements per path.

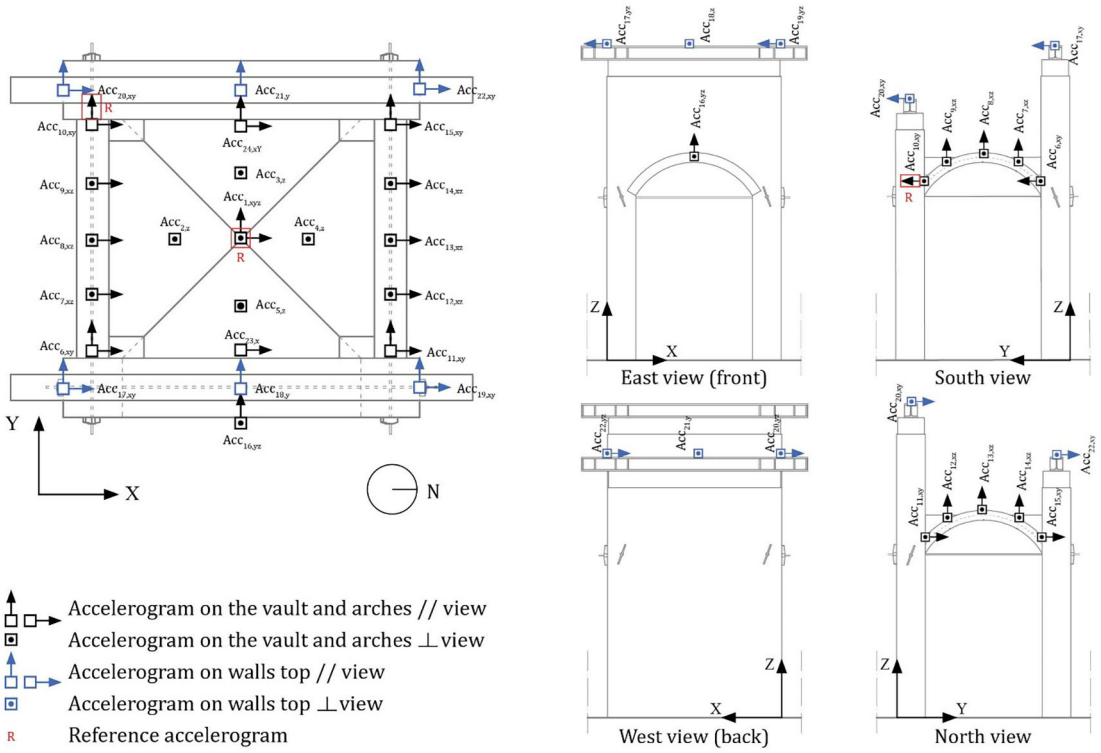


Figure 7. Instrumentation layout and accelerometer positions.

was selected to reproduce the differential seismic displacements of the two walls, thus activating the in-plane shear mechanisms in the cross vault.

The following sections provide a detailed description of the actuator configuration, control strategy, instrumentation layout, and loading protocol.

Set-up and instrumentation

This section describes the actuators employed in the experimental setup, including their functional roles and technical specifications, as well as the instrumentation used to monitor displacements and forces during testing.

Schematic views of the test set-up, the orientation of the specimen (having the reaction wall on the west side), and the labels of the structural elements are presented in Figure 11. All the actuators were attached to the rigid steel beams bolted at the top of two stone masonry walls (i.e. Wall 1 and Wall 2 on the east and west side, respectively). Each interface beam connected five actuators used to apply both the vertical permanent load (counteracted by the foundation) and the horizontal seismic action (counteracted by the lab strong-wall), as well as to apply the selected boundary conditions. In more detail, for every wall:

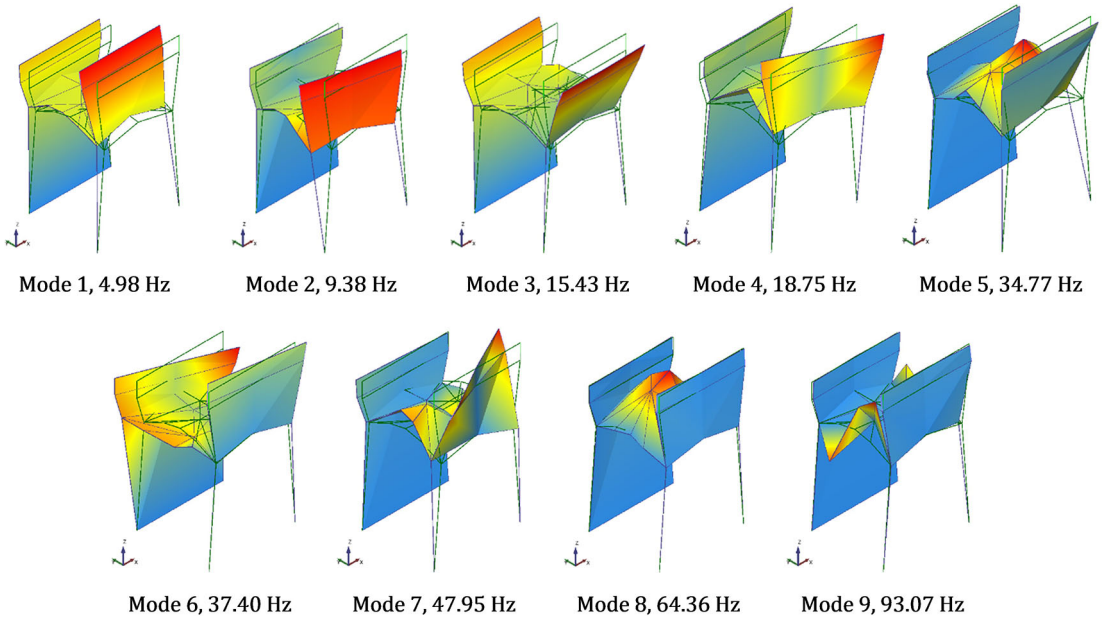


Figure 8. Identified vibration modes of the as-built configuration of the specimen from dynamic identification tests.

- 3 actuators laying in the horizontal plane controlled the horizontal co-ordinates, longitudinal south-to-north (X) translation, transversal east-to-west (Y) translation and rotation about the vertical axis (RZ);

- 2 actuators mounted vertically at the north and south ends of the beam controlled the vertical load and the rotation around the Y axis (for Wall 1) or the vertical load and the moment around the Y axis (for Wall 2).

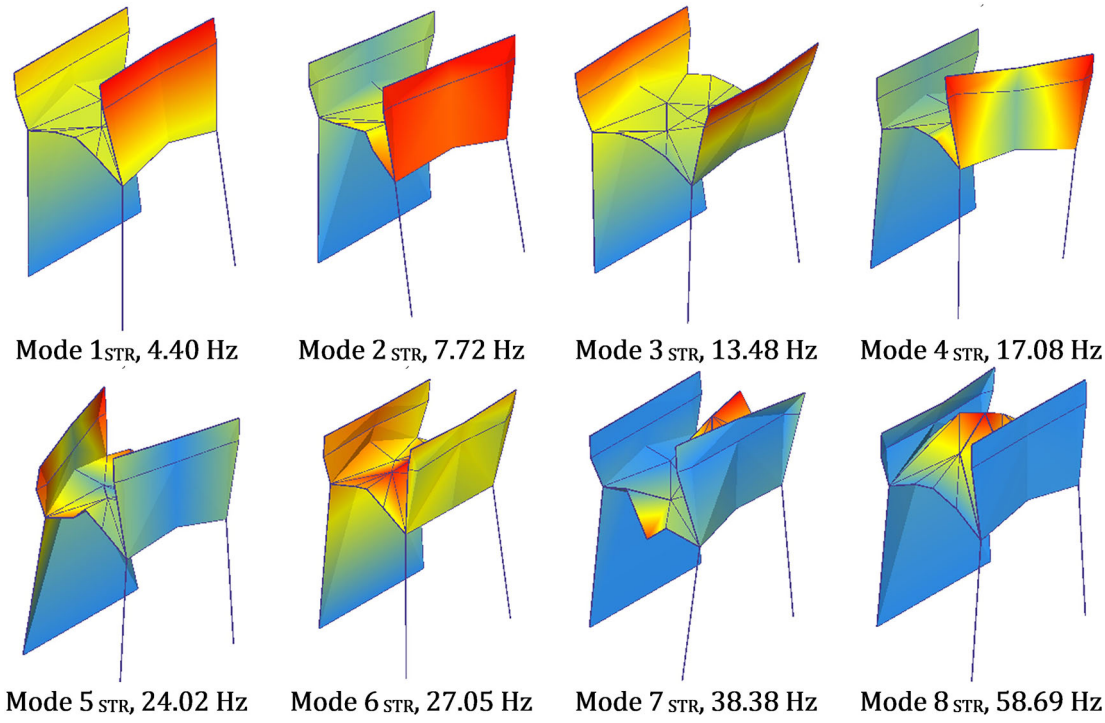


Figure 9. Identified vibration modes of the strengthened configuration of the specimen from dynamic identification tests.

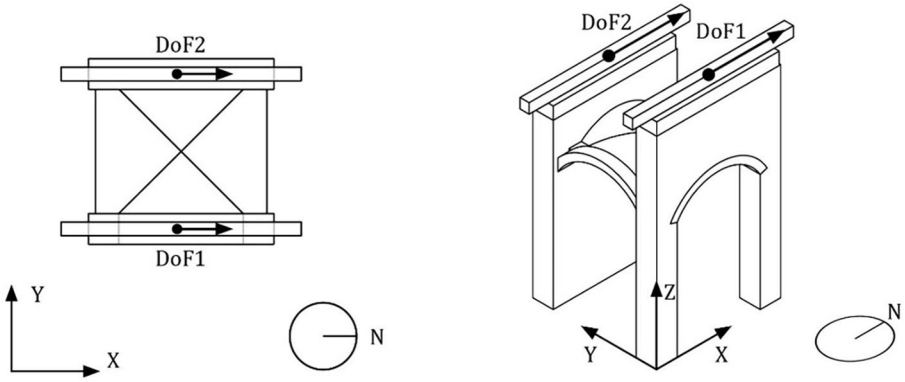


Figure 10. **Location of DoF1 and DoF2 selected for the PsD test.**

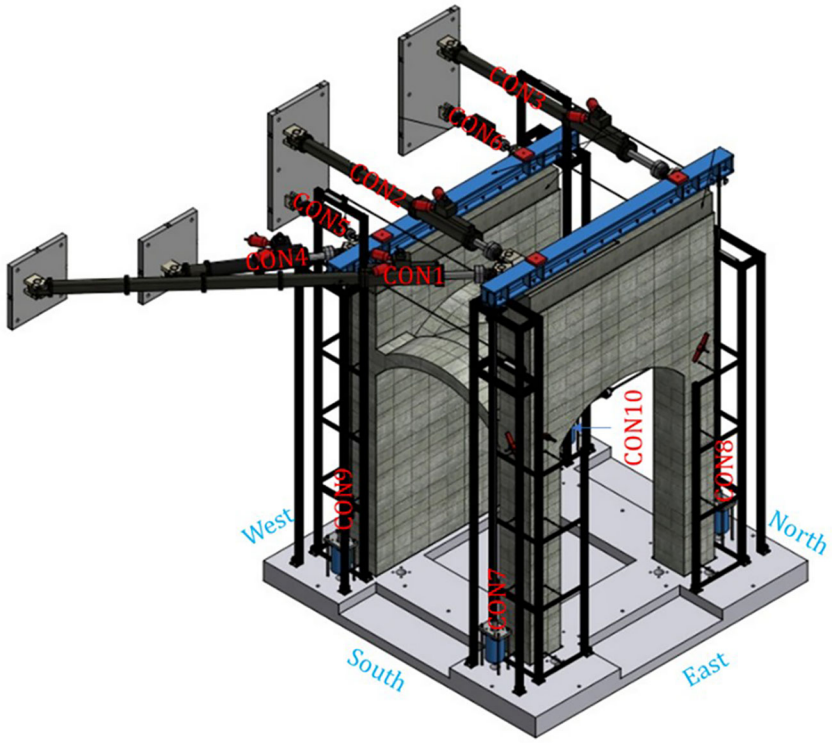


Figure 11. **Schematic view of the specimen, including orientation, actuators label.**

Next Table 3 gathers the main characteristics of the 10 installed actuators, while Table 4 lists the variables of the actuator co-ordinate system and Table 5 the ones relative to the modal-control co-ordinate system. Table 5 also includes the actuators involved in the control of each DoF and the variable chosen for the control. The labels adopted to identify each variable are set according to the nomenclature reported in the following:

- magnitude:
  - o *d* identifies a displacement (or rotation) quantity;
  - o *f* identifies a force (or moment) quantity;

- apex:
  - o *apex P* refers to the piston quantities, i.e. in the direction of each actuator.
  - o *apex M* refers to the control-mode quantities, i.e. in the XYZ reference system;
- first subscript:
  - o *k* identifies quantities related to the horizontal XY plane of Wall 1;
  - o *l* identifies quantities related to the horizontal XY plane of Wall 2;
  - o *m* identifies quantities related to the vertical XZ plane of Wall 1;
  - o *n* identifies quantities related to the vertical XZ plane of Wall 2;
- second subscript for actuator co-ordinates:
  - o *e*, *f* and *g* refer to the internal order of the horizontal actuator set (both for Wall 1 and Wall 2);
  - o *e* and *f* refer to the internal order of the vertical actuator set (both for Wall 1 and Wall 2);
- second subscript for control mode co-ordinates:
  - o *x*, *y* and Θ refer to the translational and rotational control modes in the horizontal plane (both for Wall 1 and Wall 2);
  - o *z* and *β* refer to the translational and rotational control modes in the vertical XZ plane (both for Wall 1 and Wall 2).

For the sake of clarity, two examples are given: $d^{M}_{k\Theta}$ is the control-mode rotational displacement (i.e. rotation about Z axis) at the top of Wall 1; f^{M}_{nz} is the control-mode force along Z axis at the top of Wall 2 (i.e. compression on Wall 2).

During the experiments the specimen was monitored by several instruments. Each actuator includes an embedded displacement sensor (Temposonics) and a load cell, measuring the displacement and applied load in the direction of the actuators. Clearly, such quantities need to be combined to obtain the corresponding quantities in the XYZ reference system, in which the control-mode quantities are considered. Additionally, ten displacement sensors (optical linear encoders, Heidenhain MSA 375) connected to a reference frame were monitoring the motion of the specimen at the actuators location along the XYZ reference system. Practically speaking, these instruments were mounted parallel to the actuators, with the exception of CON1 and CON4; for these last two, the sensors were mounted along the X axis, hence

Table 3. Characteristics of actuators installed on the specimen.

Label	Total stroke [mm]	Maximum force [kN]	Position
CON 1	1000	± 500	Wall 1 horizontal
CON 2	1000	± 500	Wall 1 horizontal
CON 3	1000	± 500	Wall 1 horizontal
CON 4	500	± 500	Wall 2 horizontal
CON 5	250	± 190	Wall 2 horizontal
CON 6	250	± 190	Wall 2 horizontal
CON 7	230	± 780 (*)	Wall 1 vertical
CON 8	230	± 780 (*)	Wall 1 vertical
CON 9	230	± 780 (*)	Wall 2 vertical
CON 10	230	± 780 (*)	Wall 2 vertical

**Note*: actuators 7 to 10 could apply only downward forces because of their type of connection.

Table 4. Piston co-ordinate system.

Piston co-ordinate	Displacement quantity	Force quantity	Direction	Position
CON1	d^{P}_{ke}	f^{P}_{ke}	Pulling along the actuator axis	Wall 1 horizontal
CON2	d^{P}_{kf}	f^{P}_{kf}	Pulling along the actuator axis	Wall 1 horizontal
CON3	d^{P}_{kg}	f^{P}_{kg}	Pulling along the actuator axis	Wall 1 horizontal
CON4	d^{P}_{le}	f^{P}_{le}	Pulling along the actuator axis	Wall 2 horizontal
CON5	d^{P}_{lf}	f^{P}_{lf}	Pulling along the actuator axis	Wall 2 horizontal
CON6	d^{P}_{lg}	f^{P}_{lg}	Pulling along the actuator axis	Wall 2 horizontal
CON7	d^{P}_{me}	f^{P}_{me}	Pulling along the actuator axis	Wall 1 vertical
CON8	d^{P}_{mf}	f^{P}_{mf}	Pulling along the actuator axis	Wall 1 vertical
CON9	d^{P}_{ne}	f^{P}_{ne}	Pulling along the actuator axis	Wall 2 vertical
CON10	d^{P}_{nf}	f^{P}_{nf}	Pulling along the actuator axis	Wall 2 vertical

directly measuring d^{M}_{kx} and d^{M}_{lx} displacements. All of these displacement and force sensors follow the numbering of the actuators.

During the tests, the movements of the specimen were also monitored using potentiometer displacement transducers (Gefran 50 mm and 100 mm) placed close to the four corners of the specimen along both X and Y directions. Additionally, three potentiometers on both the north and south arches were recording their vertical motions. Finally, the tensile force applied by the arches' ties was monitored by load cells (HBM) mounted at mid-length. Next Figure 12 schematically shows the position of the sensors mounted on the specimen, while gathers the complete list of sensors summarising their labels, types, ranges, monitored element, monitored side or direction, and mounting position. Note that the labels of the instruments include most of the information shown by Table 6 being, in most cases, formed by joining:

- the type of instrument (potentiometer POT or load cell LC);
- the monitored element (named according to Figure 12, e.g. P1, W2N, A1, etc.);
- the monitored side (i.e. N, S, E, W) only for the vertical elements;
- the mounting position along the length of the element:
  - o height for the vertical elements in thirds (i.e. 0 to 3);
  - o the side for the arches (i.e. west W, middle M or east E), the sensors are mounted at the quarters of the length of the elements.

For the sake of clarity and simplicity of understanding, a few examples are given in the following:

- POT_P1_S_1: potentiometer monitoring pillar P1, mounted on the south side at 1/3 of the height of the element;
- LC_A1: load cell monitoring the tie of south arch A1;
- POT_W2N_W_2: potentiometer monitoring the north end of Wall 2, mounted on the north side at 2/3 of the height of the element;
- POT_A3_W: potentiometer monitoring the north arch A3, mounted on the west side (at 1/4 of its length).

Please note that the calibration reports of all force and displacement sensors are included in the dataset. For additional details about the interpretation of the calibration reports, the reader can refer to the Technical Report No JRC139347.[7]

Table 5. Modal-control co-ordinate system.

Mode	Displacement (rotation) quantity	Force quantity	Direction	Position	Involved actuators	Controlled variable	PsD DoF or Boundary Condition (BC)
1	d^M_{kx}	f^M_{kx}	X	Wall 1 horizontal	CON1, CON2, CON3	d^M_{kx}	PsD DoF1
2	d^M_{ky}	f^M_{ky}	Y	Wall 1 horizontal	CON1, CON2, CON3	d^M_{ky}	BC: set constant equal to 0
3	$d^M_{k\Theta}$	$f^M_{k\Theta}$	Z (Θ)	Wall 1 horizontal	CON1, CON2, CON3	$d^M_{k\Theta}$	BC: set constant equal to 0
4	d^M_{lx}	f^M_{lx}	X	Wall 2 horizontal	CON4, CON5, CON6	d^M_{lx}	PsD DoF2
5	d^M_{ly}	f^M_{ly}	Y	Wall 2 horizontal	CON4, CON5, CON6	d^M_{ly}	BC: set constant equal to 0
6	$d^M_{l\Theta}$	$f^M_{l\Theta}$	Z (Θ)	Wall 2 horizontal	CON4, CON5, CON6	$d^M_{l\Theta}$	BC: set constant equal to 0
7	d^M_{mz}	f^M_{mz}	-Z	Wall 1 vertical	CON7, CON8	f^M_{mz}	BC: set constant equal to 200 kN
8	$d^M_{m\beta}$	$f^M_{m\beta}$	-Y (-β)	Wall 1 vertical	CON7, CON8	$d^M_{m\beta}$	BC: set constant equal to 0
9	d^M_{nz}	f^M_{nz}	-Z	Wall 2 vertical	CON9, CON10	f^M_{nz}	BC: set constant equal to 20 kN
10	$d^M_{n\beta}$	$f^M_{n\beta}$	-Y (-β)	Wall 2 vertical	CON9, CON10	$f^M_{n\beta}$	BC: set constant equal to 0

During the tests, ELSAREC, the ELSA REal-time Controller (for further details, refer to[8]), was used to monitor the response of the whole testing setup running multiple acquisitions in parallel. This includes signals of the standard instruments (i.e. potentiometers and load cells) as well as signals from the control system (e.g., actuator and control variables). Some continuous acquisitions were running at 10 Hz, while some others (record average) were sampled at a variable rate. These last acquisitions recorded the average values available at the conclusion of each step (record) of the loading pattern. During the pseudo-dynamic tests, for the variables involved in the equation of motion, only the record average acquisition is available. It has to be noted that the prototype-time variable, common to both acquisition files, can be used for synchronisation purposes. For further detail, refer to the Technical Report No JRC141264.[9]

Besides all the instruments mentioned above, the east side of the specimen and the intrados of the vault were monitored using stereo Digital Image Correlation (DIC). For the east façade, two digital cameras controlled and synchronised by ELSAREC, acquired high resolution photographs at regular time intervals. For the intrados, four digital cameras (organised in two independent stereo camera sets) were positioned at ground level on vault edges to monitor the northern and southern sections of the vault footprint. This allowed the recording of the whole intrados at a regular frequency of 0.25 Hz during the whole test campaign. By cross-correlating images between cameras and through time, this contactless measuring technique is able to reconstruct 3D dimensional geometry of the vault and its displacement fields. This allows tracking the formation and propagation of cracks during the experiment. Figure 13 shows the south-east side of the specimen with the random speckle patterns used by the DIC technique to track displacements. Note that the DIC images will be stored in a separate public dataset that will be published in the near future (when available, the link to this second dataset gathering DIC images only will be added on the ERIES-REVAULTs dataset object of this paper).

Test programme and loading input

As mentioned in the previous sections, the experimental campaign involved two testing phases: first, the specimen was tested in its as-built configuration, then it was repaired and reinforced using steel fibres reinforced grout, and finally it was retested in the retrofitted configuration.

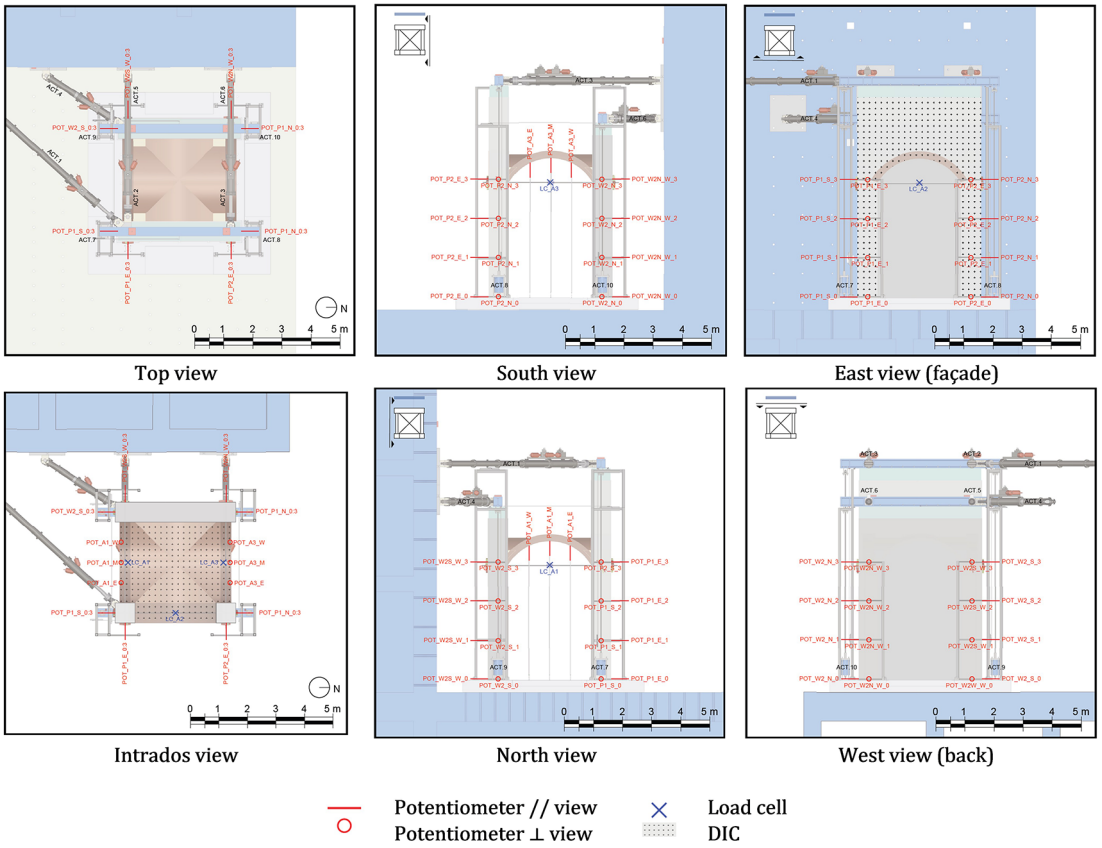


Figure 12. **Schematic view position of installed instruments.**

Table 6. **List of sensors installed on the specimen.**

Label	Type	Range	Element	Side/ Direction	Mounting position
POT_P1_S_0	Potentiometer	50 mm	Pillar P1	South/X	0 (Base)
POT_P1_S_1	Potentiometer	100 mm	Pillar P1	South/X	1/3 of height
POT_P1_S_2	Potentiometer	100 mm	Pillar P1	South/X	2/3 of height
POT_P1_S_3	Potentiometer	100 mm	Pillar P1	South/X	3/3 of height
POT_P1_E_0	Potentiometer	50 mm	Pillar P1	East/Y	0 (Base)
POT_P1_E_1	Potentiometer	100 mm	Pillar P1	East/Y	1/3 of height
POT_P1_E_2	Potentiometer	100 mm	Pillar P1	East/Y	2/3 of height
POT_P1_E_3	Potentiometer	100 mm	Pillar P1	East/Y	3/3 of height
POT_P2_N_0	Potentiometer	50 mm	Pillar P2	North/X	0 (Base)
POT_P2_N_1	Potentiometer	100 mm	Pillar P2	North/X	1/3 of height
POT_P2_N_2	Potentiometer	100 mm	Pillar P2	North/X	2/3 of height
POT_P2_N_3	Potentiometer	100 mm	Pillar P2	North/X	3/3 of height
POT_P2_E_0	Potentiometer	50 mm	Pillar P2	East/Y	0 (Base)
POT_P2_E_1	Potentiometer	100 mm	Pillar P2	East/Y	1/3 of height
POT_P2_E_2	Potentiometer	100 mm	Pillar P2	East/Y	2/3 of height
POT_P2_E_3	Potentiometer	100 mm	Pillar P2	East/Y	3/3 of height

Table 6. *Continued*

Label	Type	Range	Element	Side/ Direction	Mounting position
LC_A1	Load cell	±125 kN	Tie on arch A1	- /Axial	Middle
LC_A2	Load cell	±125 kN	Tie on arch A2	- /Axial	Middle
LC_A3	Load cell	±125 kN	Tie on arch A3	- /Axial	Middle
POT_W2N_N_0	Potentiometer	50 mm	Wall 2 North end W2N	North/X	0 (Base)
POT_W2N_N_1	Potentiometer	50 mm	Wall 2 North end W2N	North/X	1/3 of height
POT_W2N_N_2	Potentiometer	50 mm	Wall 2 North end W2N	North/X	2/3 of height
POT_W2N_N_3	Potentiometer	50 mm	Wall 2 North end W2N	North/X	3/3 of height
POT_W2N_W_0	Potentiometer	50 mm	Wall 2 North end W2N	West/Y	0 (Base)
POT_W2N_W_1	Potentiometer	50 mm	Wall 2 North end W2N	West/Y	1/3 of height
POT_W2N_W_2	Potentiometer	50 mm	Wall 2 North end W2N	West/Y	2/3 of height
POT_W2N_W_3	Potentiometer	50 mm	Wall 2 North end W2N	West/Y	3/3 of height
POT_A3_W	Potentiometer	50 mm	North arch A3	Intrados/Z	West quarter
POT_A3_M	Potentiometer	50 mm	North arch A3	Intrados/Z	Middle
POT_A3_E	Potentiometer	50 mm	North arch A3	Intrados/Z	East quarter
POT_W2S_S_0	Potentiometer	50 mm	Wall 2 South end W2S	South/X	0 (Base)
POT_W2S_S_1	Potentiometer	50 mm	Wall 2 South end W2S	South/X	1/3 of height
POT_W2S_S_2	Potentiometer	50 mm	Wall 2 South end W2S	South/X	2/3 of height
POT_W2S_S_3	Potentiometer	50 mm	Wall 2 South end W2S	South/X	3/3 of height
POT_W2S_W_0	Potentiometer	50 mm	Wall 2 South end W2S	West/Y	0 (Base)
POT_W2S_W_1	Potentiometer	50 mm	Wall 2 South end W2S	West/Y	1/3 of height
POT_W2S_W_2	Potentiometer	50 mm	Wall 2 South end W2S	West/Y	2/3 of height
POT_W2S_W_3	Potentiometer	50 mm	Wall 2 South end W2S	West/Y	3/3 of height
POT_A1_W	Potentiometer	50 mm	South arch A1	Intrados/Z	West quarter
POT_A1_M	Potentiometer	50 mm	South arch A1	Intrados/Z	Middle
POT_A1_E	Potentiometer	50 mm	South arch A1	Intrados/Z	East quarter

The shared data belong to both phases, each of them includes a preliminary pseudo-static test, useful for the determination of the initial stiffness, and several Pseudo-Dynamic (PsD) hybrid experiments at increasing amplitude.

Table 7 summarises the complete list of experiments origin of the data included in the dataset.

The input accelerogram was introduced in the X direction for the PsD tests and was derived from the ground motion record of L'Aquila earthquake (6th of April 2009 – AQA; L'Aquila – v. Aterno – F. Aterno). The original accelerogram duration was cropped from 25 s to approximately 10 s, to limit the overall test duration. Figure 14 shows the input accelerogram adopted as input for the PsD tests, also including the zero padding on the last 0.5 s included to set the specimen in free vibration. The original sampling of the accelerogram was 0.05 s of prototype time, but for the tests it was decided to use a resampled version (through linear interpolation) with a sampling of 0.001 s. Using the continuous PsD method at ELSA, the prototype time input increment (Recording Increment of 0.001 s) is subdivided for the integration in

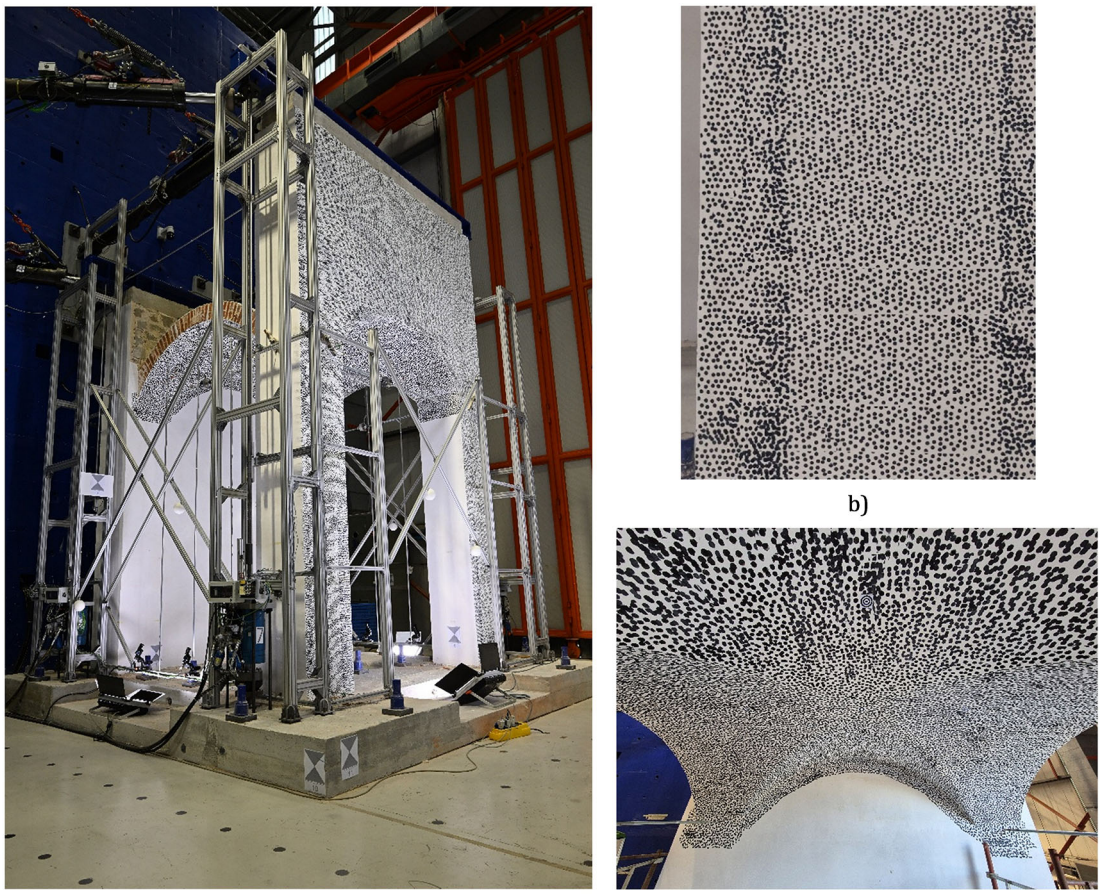


Figure 13. **View of the specimen (a) and the random speckle pattern applied for DIC: b) east façade; c) intrados.**

Table 7. **List of performed experiments.**

Experiment tag	Description	Maximum amplitude	Specimen configuration
c01	Cyclic (determination of stiffness)	1 mm	As-built
c05	Pseudo-Dynamic	10%	As-built
c06	Pseudo-Dynamic	25%	As-built
c07	Pseudo-Dynamic	75%	As-built
c08	Pseudo-Dynamic	100%	As-built
c09	Pseudo-Dynamic	125%	As-built
c10	Pseudo-Dynamic	150%	As-built
d02	Cyclic (determination of stiffness)	1 mm	Retrofitted
e01	Pseudo-Dynamic	25%	Retrofitted
e02	Pseudo-Dynamic	75%	Retrofitted
e03	Pseudo-Dynamic	100%	Retrofitted
e04	Pseudo-Dynamic	125%	Retrofitted
e06	Pseudo-Dynamic	150%	Retrofitted

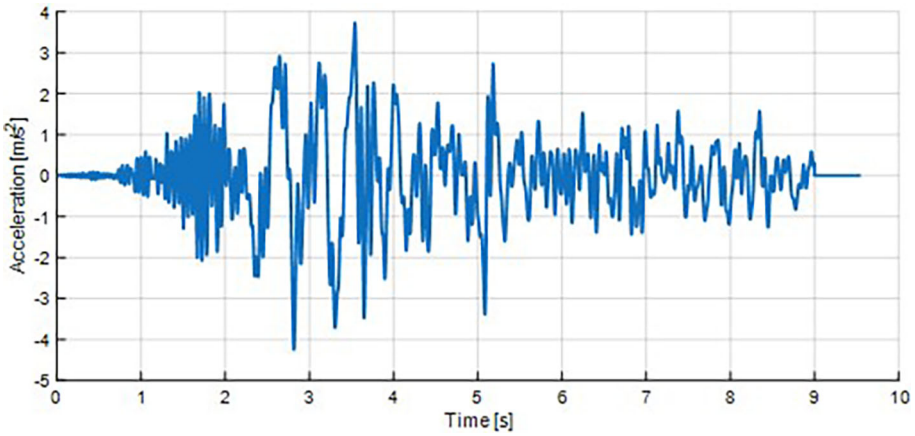


Figure 14. Acceleration time-history input of the PsD tests (100% intensity).

a number of internal time increments (InterRec = 500 in this case) but only the average value of every variable is saved for every Recording Increment.

A lumped mass matrix was used for the equation of motion with masses of 21569 and 8071 kg associated, respectively, to the DoFs of Wall1 and Wall 2 in the X direction

Conclusions

This paper presents the dataset generated within the ERIES-REVAULTs experimental campaign, which involved full-scale Pseudo-Dynamic (PsD) testing of a masonry cross-vault system representative of the lateral nave bays of historic masonry churches. The campaign was designed to investigate the in-plane shear response induced by differential longitudinal displacements of the vault supports, a damage mechanism frequently observed in post-earthquake surveys of historical masonry structures.

The shared dataset documents both the as-built and the retrofitted configurations of the specimen, the latter strengthened using a Steel-Reinforced Grout (SRG) system. This work makes available a set of full-scale experimental data on a complex masonry vaulted system tested under hybrid seismic simulation. The dataset is expected to support a wide range of future studies, including the calibration and validation of numerical models, the assessment of strengthening effectiveness, the interpretation of crack development and displacement patterns, and the comparison of alternative seismic assessment and retrofit strategies for masonry historical structures.

Ethic and consent

Ethical approval and consent were not required.

Data availability

Zenodo. REVAULTs: Response Evaluation of masonry VAULTs under pseudo-dynamic loadings: dataset

https://doi.org/10.5281/zenodo.19552030 [10].

This project contains the following underlying data:

REVAULTs_v1.zip. The zip file, once extracted, allows accessing to the whole dataset. The information is accessible to a standard filesystem structure. Due to its complexity, in order to understand the structure of the shared dataset, the reader should refer to the Technical Report No JRC141264.[9] A short list of the main contents includes (i) details of the specimens, (ii) applied loading patterns, (iii) details and calibration reports relative to the installed instrumentations (for further details on the calibration procedure, refer to the Technical Report No JRC139347[7]). Besides, for each test, the dataset includes: (i) raw data as recorded by the acquisition system of the ELSA lab, (ii) processed data for an easier access to the output of the monitoring, (iii) graphical representation of the main response quantities.

The dataset is under embargo until 30/11/2026, as provided for in the grant agreement. Data is available under the terms of the CC BY 4.0 license.

The paper briefly presents the ERIES-REVAULTs project, including all relevant information regarding the specimens, measuring equipment, test setup and test procedure. Future publications will include detailed analyses and discussion of the results. The dataset, gathering quantitative information and metadata, is made available by the authors in line with the requirement of the framework of the ERIES Project [Grant agreement ID: 101058684, https://doi.org/10.3030/101058684]. The complete dataset can be downloaded at https://doi.org/10.5281/zenodo.19552030 under a CC BY 4.0 license.

Acknowledgements

The authors acknowledge the contributions of all team members of the ERIES-REVAULTs project who are not authors of this paper. The authors are also thankful for all the help and support of the staff at the JRC ELSA facility, without whom this experimental campaign could not have been successfully completed.

References

1. Rossi M, Calderini C, Lagomarsino S: **Experimental testing of the seismic in-plane displacement capacity of masonry cross vaults through a scale model.** *Bull. Earthq. Eng.* Jan. 2016; **14**(1): 261–281. **Publisher Full Text**
2. Bianchini N, Mendes N, Calderini C, *et al.*: **Seismic response of a small-scale masonry groin vault: experimental investigation by performing quasi-static and shake table tests.** *Bull. Earthq. Eng.* Feb. 2022; **20**(3): 1739–1765. **Publisher Full Text**
3. Carfagnini C, Baraccani S, Silvestri S, *et al.*: **The effects of in-plane shear displacements at the springings of Gothic cross vaults.** *Constr. Build. Mater.* 2018; **186**: 219–232. **Publisher Full Text**
4. Silvestri S, *et al.*: **Shaking table testing of groin vaults made by 3D printers.** *Soil Dyn. Earthq. Eng.* 2021; **150**(April): 106880. **Publisher Full Text**
5. Bianchini N, Mendes N, Calderini C, *et al.*: **Shaking Table Testing of an Unstrengthened and Strengthened with Textile Reinforced Mortar (TRM) Full-Scale Masonry Cross Vault.** *International Journal of Architectural Heritage.* Dec. 2024; **18**(12): 1799–1824. **Publisher Full Text**
6. Cardani G, Rossi M, Bournas D: **Laboratory Tests for the Characterisation of a Sedimentary Arenaceous Limestone Used in the Architectural Heritage of Northern Italy.** 2026: 437–450. **Publisher Full Text**
7. Peloso S, *et al.*: *ELSA - Procedure for calibration and verification of displacement and rotation measuring systems.* Luxembourg: Publications Office of the European Union; 2024. JRC139347. **Publisher Full Text**
8. Peroni M, Pegon P, Molina FJ, *et al.*: **Ethernet-Based Servo-Hydraulic Real-Time Controller and DAQ at ELSA for Large Scale Experiments.** *J. Earthq. Eng.* Nov. 2022; **26**(15): 7657–7688. **Publisher Full Text**
9. Peloso S, Molina FJ, Lamperti Tornaghi M, *et al.*: *ELSA - Structure of the experimental datasets.* Luxembourg: Publications Office of the European Union; 2025. JRC141264. **Publisher Full Text**

Open Peer Review

Current Peer Review Status: ? ?

Version 1

Reviewer Report 13 October 2026

https://doi.org/10.21956/openreseurope.25885.r81411

© **2026 Amer O.** This is an open access peer review report distributed under the terms of the Creative Commons Attribution License, which permits unrestricted use, distribution, and reproduction in any medium, provided the original work is properly cited.

?

Osama Amer
[1] Civil Engineering, Institute for Sustainability and Innovation in Structural Engineering (Ringgold ID: 451178), Guimarães, Portugal
[2] Cairo University / Ain Shams University, Cairo, Cairo Governorate, Egypt

This paper presents an experimental dataset from a Pseudo-Dynamic test on a masonry cross-vault system representing an intermediate bay of a historic church. The study evaluates the in-plane shear response of the vault under differential support displacements in both as-built and SRG-retrofitted configurations. The topic is of significant interest to the structural engineering community for understanding vault-substructure seismic interaction. However, several critical areas require revision before the manuscript can be considered for indexing. The following revisions are recommended:

1. Condensing the equation of motion into two horizontal masses neglects vertical web acceleration, which governs horizontal thrust variation and line-of-thrust shifting that drives crown cracking. The authors must justify this simplification and address its impact on the observed failure mode.
2. The damping matrix is undefined. Initial-stiffness Rayleigh damping in cracking masonry produces artificial forces across open cracks. The authors must specify the damping formulation, report the modal damping ratios and confirm whether spurious damping affected the high-amplitude response.
3. The retrofit was tested on a on a heavily damaged specimen to 150% PGA. Crack grouting cannot eliminate internal shear-slip along bed joints or residual offsets, so Phase 2 assesses a repaired (not pristine) structure. The authors must report residual plastic displacements after post-test and review the framing of Phase 2 (I think it may be framed as post-earthquake rehabilitation).
4. I strongly advise the authors to reconsider explaining the underlying mechanisms regarding the modal frequency drop post-strengthening and the Mode 5/6 inversion. This seems to be strongly related to the current study.
5. Critical constitutive interface parameters are missing. The authors must provide the mortar-unit joint cohesion and friction angle, the SRG-to-brick debonding fracture energy, and the initial pre-tension forces in tie-rods.

6. For the dynamic Young's moduli in Table 2, the authors must report the assumed Poisson's ratio and density used in the calculations, and state whether a 1D rod or 3D continuum velocity was assumed.
7. The dataset is listed as under embargo on Zenodo until 30/11/2026. As a result, it was not possible to access it to verify the data structure, metadata, or raw records.

Is the rationale for creating the dataset(s) clearly described?
Yes

Are the protocols appropriate and is the work technically sound?
Yes

Are sufficient details of methods and materials provided to allow replication by others?
Partly

Are the datasets clearly presented in a useable and accessible format?
No

Competing Interests: No competing interests were disclosed.

Reviewer Expertise: Numerical Modelling & FEA: Non-linear finite element analysis (DIANA FEA, ABAQUS, ANSYS) of concrete, steel, and masonry structures.Composite & Reinforced Concrete Structures: Behaviour of FRP- and steel-reinforced concrete elements, cyclic/seismic performance, and novel composite/sandwich panel systems.Structural Assessment, Retrofitting & Conservation: Diagnosis, retrofitting, and strengthening of historical masonry and reinforced concrete structures.Experimental Mechanics: Quasi-static cyclic testing, shear walls, columns, and materials characterization.

I confirm that I have read this submission and believe that I have an appropriate level of expertise to confirm that it is of an acceptable scientific standard, however I have significant reservations, as outlined above.

Reviewer Report 21 September 2026

https://doi.org/10.21956/openreseurope.25885.r80768

© 2026 Porcu M. This is an open access peer review report distributed under the terms of the Creative Commons Attribution License, which permits unrestricted use, distribution, and reproduction in any medium, provided the original work is properly cited.

?

Maria Cristina Porcu
University of Cagliari, Cagliari, Italy

Summary. This paper deals with an experimental campaign conducted on a full-scale masonry cross vault that was constructed in a laboratory setting and subjected to pseudo-dynamic testing. The research involved academics from several universities and research institutes. The purpose of

the authors was to provide a test procedure for investigating the in-plane shear behaviour of masonry cross vaults under differential longitudinal displacements of the supports caused by seismic actions. A full-scale masonry cross vault, including also two frontal piers and a back wall, was built in a laboratory. The as-built vault and the vault strengthened with a steel-reinforced grout (SRG) system were both investigated under seismic action. The study provides useful information on the test equipment and procedures for this type of experimental investigation. Masonry cross vaults are a common feature of historic buildings, such as churches and monasteries. One of the most common causes of damage to these structural features is earthquakes. However, a full understanding of the dynamic behaviour of masonry vaults remains elusive. Therefore, the present study could make a significant contribution to the field.
Overall, the manuscript is well written and organized. It provides detailed information on the specimen, materials, laboratory setup, instrumentation, and loading protocols, enabling the tests to be replicated. Data obtained from testing the as-built and strengthened specimens are available via a link. However, there is no presentation or discussion of the results in the manuscript. The paper is intended to present only the experimental protocol. According to the authors, the originality of the study with respect to other similar literature investigations lies in considering also piers and a perimetral wall in the laboratory specimen.

According to the comments below, there are some major and minor improvements that could be made.

1. The actuators were bolted to the steel beams at the top of the masonry walls. However, seismic action occurs at foundation level. Does the test simulate the effect of the rest of the structure on the vault? If so, applying an earthquake at the top level would not be entirely accurate. Most of the papers cited in the manuscript, in fact, carried out shaking table tests, where the earthquake was applied at the base of the structure, cf. e.g.
2. [Ref 1], [Ref 2], [Ref 3].
3. Some doubts arise. The choice of the loading setup should be better justified in the manuscript. How and why can an earthquake apply at the top level reproduce the effects of in-situ seismic actions? The authors should address this issue.
4. The vertical component of the earthquake seems not to be considered in the study. However, it could affect the in-plane behaviour. This choice should be justified.
5. Typically, two horizontal components of an earthquake are applied in both numerical and experimental tests. Why are actuators CON1 and CON 4 inclined with respect to the walls? Actuators 2, 3, 5, and 6 simulate the out-of-plane action of the earthquake on the walls (y direction). Instead, in-plane action in the x-direction is not directly simulated. Some comments could help to better understand this setup choice.
6. Presenting and commenting on the results of the proposed experimental procedure (or at least some of them) would enhance the research and add value to the paper. Failing to present these results could be perceived as a weakness.
7. The frequencies of the strengthened configuration are lower than those of the as-built configuration. The strengthened configuration, however, is expected to be stiffer, and thus to have lower natural frequency values. 'Why does this occur?' Was the as-built specimen sensibly damaged after testing? It is worth making some comments on modal comparison, since these two configurations are in fact the focus of the study.
8. Page. 6, Line 2. Please avoid repetition of “carried out” in the same sentence. The sentence could be replaced, for instance, by “The structural strengthening intervention was carried out in mid-January 2026, after the first set of PsD tests.”
9. Page. 15: Improve the sentence “Figure 14 shows the input accelerogram adopted as input

for the PsD tests,...", where the word "input" appears twice.
10. For the purposes of coherence and comparison, the size of the mode shapes presented in Figure 9 should be analogous to that in Figure 8.
11. Page. 17. The last sentence before the Conclusions ("A lumped mass matrix was used for the equation of motion with masses of 21569 and 8071 kg associated, respectively, to the DoFs of Wall1 and Wall 2 in the X direction") appears inconsistent with the rest of the paper. It could be related to a numerical model that is, however, not presented in the manuscript.
12. The Introduction could be improved and the Bibliography expanded by presenting the state of the art more effectively.

References

1. Bianchini N, Mendes N, Calderini C, Candeias P, et al.: Seismic response of a small-scale masonry groin vault: experimental investigation by performing quasi-static and shake table tests. *Bulletin of Earthquake Engineering*. 2022; **20** (3): 1739-1765 Publisher Full Text
2. Silvestri S, Baraccani S, Foti D, Ivorra S, et al.: Shaking table testing of groin vaults made by 3D printers. *Soil Dynamics and Earthquake Engineering*. 2021; **150**. Publisher Full Text
3. Bianchini N, Mendes N, Calderini C, Candeias P, et al.: Shaking Table Testing of an Unstrengthened and Strengthened with Textile Reinforced Mortar (TRM) Full-Scale Masonry Cross Vault. *International Journal of Architectural Heritage*. 2024; **18** (12): 1799-1824 Publisher Full Text

Is the rationale for creating the dataset(s) clearly described?

Partly

Are the protocols appropriate and is the work technically sound?

Partly

Are sufficient details of methods and materials provided to allow replication by others?

Yes

Are the datasets clearly presented in a useable and accessible format?

No

Competing Interests: No competing interests were disclosed.

Reviewer Expertise: Dynamics of Structures; Masonry arched and vaulted structures; Seismic Analyses; Experimental tests and numerical models; Modal tests.

I confirm that I have read this submission and believe that I have an appropriate level of expertise to confirm that it is of an acceptable scientific standard, however I have significant reservations, as outlined above.